Zooming out: what a broader view is telling us about stellar and substellar conglomerates

K. Peña Ramírez[1]

[1] *Centro de Astronomía (CITEVA), Universidad de Antofagasta, Chile*

Contacto / karla.pena@uantof.cl

Resumen / La medición de distribuciones de edades y masas de estrellas de baja masa y objetos subestelares en diversos ambientes jóvenes requiere de un censo minucioso de esta población en particular. Tradicionalmente, los estudios que se llevan a cabo en este sentido buscan miembros en conglomerados definidos usando rasgos de juventud (variabilidad, líneas de emisión, exceso de emisión infrarroja, emisión en rayos X), movimientos propios y diagramas color-magnitud en el óptico y el infrarrojo. Dado el acceso a los más recientes relevamientos de cielo completo, se cuenta ahora con un mayor número de objetos bajo estudio y una serie de desafíos teóricos y observacionales se mantienen latentes dentro del campo. La definición de funciones de luminosidad en conglomerados delineados sufre modificaciones ante un cubrimiento espacial mayor y homogéneo de su población de objetos ultra fríos. Algunos ejemplos recientes son presentados.

Abstract / Measuring the distributions of ages and masses of low-mass stars and substellar sources in different young environments requires a thorough census of this specific population. Typically, studies have searched for defined conglomerate members using signatures of youth (variability, emission lines, infrared (IR) excess emission, X-ray emission), proper motions, and optical and near-IR color-magnitude diagrams. Given the access to the most recent all-sky surveys, better statistics are now in place, and a series of observational and theoretical challenges keep the field ongoing. Given a wider and uniform spatial coverage of ultra-cool dwarf sources, the diversity of spatial structures and the traditional definition of luminosity functions in spatially-delineated conglomerates should be revisited. Some recent examples are presented.

Keywords / open clusters and associations — stars: kinematics and dynamics — stars: pre-main sequence

1. Introduction

With the advent of large photometric/astrometric/spectroscopic surveys, the panorama of the physical processes beneath the formation and dynamics of low mass stars and massive brown dwarfs has changed radically. The low mass population of our Milky Way is mainly populated by ultra-cool dwarfs being the bridges between the stellar and the substellar population of the Galaxy. There are not only new insights about the specific features relevant to the stellar/substellar transition but in the definitions of the environments where these kinds of sources lie. The defining boundaries of star-forming regions, open clusters, associations, moving groups at ages of less than a few Myr are no longer clear, making even harder to arise conclusions of a specific population in a determined spatial portion of space.

2. Spatial location

Ultra-cool dwarfs (sources of about M7 spectral type or later) have been found mainly as field old dwarfs, young members of star-forming regions, clusters and associations as well as members of young moving groups. In terms of detected ultra-cool dwarfs as not members of gravitationally bound structures, before Gaia Data Release 2 (DR2, Gaia Collaboration et al., 2018) the number of known dwarfs in the field was about 4300. This number has increased considerably with recent works using Gaia data. One example is the photometric selection done by Reylé (2018), in which the number of filed ultra-cool dwarfs would rise to more than 13 700 sources. Even more, the discovery of three L-type dwarfs at about 10-19 pc (Scholz & Bell, 2018) suggests that there exist remaining undiscovered objects in this volume.

The census of ultra-cool dwarfs in very young star-forming regions has been reaching a few Jupiter masses in several locations: λ Orionis (e.g., Barrado y Navascués et al., 2007; Bayo et al., 2011); NGC 1333 (e.g., Scholz et al., 2009, 2012; Luhman et al., 2016); IC 348 (e.g., Alves de Oliveira et al., 2013; Burgess et al., 2009; Luhman et al., 2016); σ Orionis (e.g., Zapatero Osorio et al., 2000; Caballero et al., 2007; Bihain et al., 2009; Peña Ramírez et al., 2011, 2012, 2015); Orion Nebular Cluster (e.g., Lucas et al., 2001; Weights et al., 2009; Hillenbrand et al., 2013; Ingraham et al., 2014; Suenaga et al., 2014), ρ Ophiuchus (e.g., Geers et al., 2011; Mužić et al., 2012; Alves & Bouy, 2012; Chiang & Chen, 2015); Upper Scorpius (e.g., Ardila et al., 2000; Slesnick et al., 2006; Peña Ramírez et al., 2016; Best et al., 2017; Lodieu et al., 2018); 25 Orionis (e.g., Suárez et al., 2017); Taurus (e.g., Luhman et al., 2006; Slesnick et al., 2006; Esplin et al., 2017; Luhman, 2018), among others. Being this kind of environments the most suitable ones to pursue studies on the formation and evolution of ultra-cool dwarfs given the premise of a common origin for all the cloud members.

Low mass dwarfs have also been reported as members of co-moving groups. Now, we count with low mass populations of various young moving groups as close as ∼150 pc. Given that these are sparse, low-density populations the membership studies and age assessment of the low mass content of young moving groups is a demanding task. Recent studies suggest that there are about 900 ultra-cool dwarfs of spectral types as late as L2 in the seven nearest young co-moving groups (Gagné & Faherty, 2018).

3. Challenges

Given the increased amount of observational data, the field has faced a series of challenges trying to reconcile not only all the observational efforts among themselves but also to give an appropriate theoretical description of the physical processes beneath the formation and evolution of the low mass stellar/substellar galactic population.

In that sense, there has been a vast improvement from the first evolutionary models (e.g., Baraffe et al., 1998) describing the mass regime of about 0.075 to 1 $M_\odot$ (not even describing the massive extreme of the substellar regime) at optical wavelengths and using the interior physics and non-grey atmosphere models available at the time. Missing sources of opacity in the optical together with the limited treatment of grain formation accounted for some of the discrepancies among observational sequences and theoretical isochrones. We do count now, twenty years later, with models with updated molecular lists, updated solar abundances, and the inclusion of atmospheric convection parameters calibrated on 2D/3D radiative hydrodynamics simulations in the near infrared (e.g., Baraffe et al., 2015). An example of the improvement can be seen in Fig 1 where the σ Orionis cluster sequence (Peña Ramírez et al., 2012) is compared with the set isochrones of Baraffe et al. (1998) and Baraffe et al. (2015). The new set of isochrones and the observational sequence are in agreement specially for the massive brown dwarfs in the cluster. The situation becomes worse for the faintest sources, in particular in the $J-K$ color, possibly related with the presence of infrared excesses due to circun(sub)stellar disk of these young sources.

A similar panorama faces the theoretical work of synthetic spectra of ultra-cool dwarfs. There have been tremendous efforts in the modeling of atmosphere models and the derivation of synthetic spectra. The BT-Settl (Allard et al., 2012; Allard, 2014) synthetic spectra, for example, aim to describe the atmospheres of low-mass stars, brown dwarfs, and planets without irradiation. They include a cloud model by accounting for the formation and gravitational settling of dust grains for $T_{\rm eff} \leq 2700$ K. As can be seen in Fig.2 the over-all aspect of the optical and near-infrared data is successfully reproduced by the theoretical spectra, implying that no relevant molecule or atomic element is missing from the atmospheric computations. Synthetic spectra still face limitations on reproducing specific spectroscopic features of ultra-cool dwarfs in part due to the limited signal

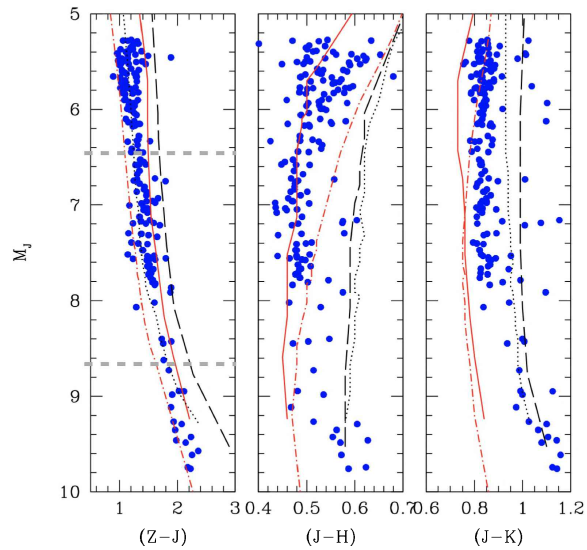

Figura 1: Comparison of models with observations in the σ Orionis cluster in various color-magnitude diagrams. Isochrones of 1 Myr and 10 Myr are displayed for various sets of models. Baraffe et al. (2015) (red): solid (1 Myr) and dash-dot (10 Myr). Baraffe et al. (1998) models (black): long dashed (1 Myr) and dot (10 Myr). The data (blue dots) are from Peña Ramírez et al. (2012). Figure from Baraffe et al. (2015).

to noise achieved of intrinsically faint sources, even at large astronomical facilities. From Fig 2, the VO features are typically less intense in observed data, water opacities can be related with the not so accurate H-peak shape, and the noise level at K-band prevents us from comparing observations from synthetic spectra associated with the CO band. The models do reproduce the relative fluxes between the optical, J-, H-, and K-bands, which can be understood as evidence in favor of a proper treatment of the gas and dust condensation chemistry and the dust opacity at these low temperatures and surface gravities (Zapatero Osorio et al., 2017).

Different approaches have been undertaken to define a precise sequence of spectral types among low-mass dwarfs. The definition of standardized datasets either at optical or infrared wavelengths as well as the quest of homogeneity in involved instrumentation and reduction techniques has been one of the main drivers in recent works. The mentioned challenges in the atmospheres of the ultra-cool dwarfs led to several difficulties on the spectral type determination. As an example, the recent work of Luhman (2018) redefines the sequence of dwarfs entirely later than M6 spectral type in the Upper Scorpius association deriving a tighter sequence of members, including the faintest ones (Peña Ramírez et al., 2016). The comparison of dwarfs found in different environments has also been benefited from the large statistic now available. In Best et al. (2018), authors made a global comparison among different color combinations of ultra-cool dwarfs from the field, from young environments, binaries, and subdwarfs. The work mentioned above includes near ten thousand field dwarfs found in the Pan-STARRS1 3π Survey (Chambers et al., 2016). As a result, there seems to be a surprising diversity of

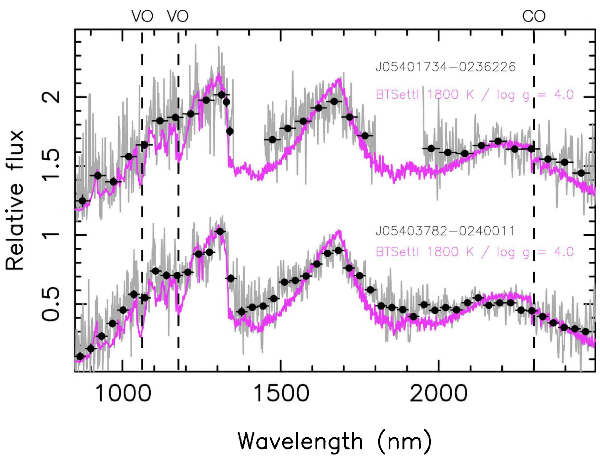

Figura 2: Best-fit BT-Settl synthetic spectra (magenta lines) plotted together with the observed spectra (gray lines) of a couple of faint σ Orionis ultra-cool dwarfs (J=19.5, 19.9 mag). The rebinned data are shown with black dots. All models are computed for solar metallicity and log g = 4.0 (cm s^{-2}). Spectra are normalized to unity at 1.28-1.32 μm and offset vertically by a constant. Figure from Zapatero Osorio et al. (2017).

L-type colors in the near infrared. Theoretically, this diversity is explained by dust dispersal that includes both a sudden sinking of the entire cloud deck into the deep, unobservable atmosphere or breakup of the cloud into scattered patches (as seen on Jupiter and Saturn, Crossfield et al. (2014)). Until recently, observations of brown dwarfs have been limited to globally integrated measurements; such measurements can reveal surface inhomogeneities but cannot unambiguously resolve surface features. Crossfield et al. (2014), presented a two-dimensional map of large scale bright and dark features possibly related to patchy clouds in the Luhman 16AB system at two pc (Luhman, 2013). This early T-dwarf presents constant temporal variability with a rotation period of $\sim$5 h, brightness variations of $\pm$10 % and even a bright spot in the pole. The work of Apai et al. (2017) presents a long-term Spitzer Space Telescope infrared monitoring campaign of three brown dwarfs to constrain cloud cover variations over a total of 192 rotations along 1.5 years. As a result, authors support the presence of zonal temperature and wind speed variations which would help to explain puzzling behaviors seen in brown dwarf brightness variations.

The mass determination of ultra-cool dwarfs is one of its biggest challenges. The work on dynamical masses of Dieterich et al. (2018) in the system ϵ Indi B and C gave us a recent example. Both sources are close to the theoretical hydrogen burning minimum mass limit a key point of transition between the stellar and the substellar regime. The reported mass for ϵ Indi B, a T1.5 dwarf, is 75$\pm$0.8 $\mathrm{M_{Jup}}$, while the mass assigned to ϵ Indi C, a T6 dwarf, is 70.1$\pm$0.7 $\mathrm{M_{Jup}}$. Given that for a mid-T dwarf its mass value can range between $\sim$20 $\mathrm{M_{Jup}}$ for a source with 500 Myr to $\sim$60 $\mathrm{M_{Jup}}$ for a source with an age of 10 Gyr; the dynamical mass values found by Dieterich et al. (2018) are extremely high. Unknown molecule and cloud formation, poor knowledge of opacities that affect the rate of cooling are among the reasons for this discrepancy. Authors claim that it is clear that the current models under-predict the upper mass limit and (or) the necessary cooling rates for ϵ Indi B and C, with less opaque models coming closer to replicating the observed parameters.

Finally, it is relevant to mention the gap observed in the Hertzsprung-Russell diagram of field early-type M dwarfs based on Gaia DR2 measurements (Jao et al., 2018). A gap introduces a diagonal feature that dips toward lower luminosities at redder colors. It is seen at various distances (<130 pc) and it is not tight to Gaia photometry. The gap is near the luminosity-temperature regime where M dwarf stars transition from partially to fully convective, i.e., near spectral type M3.0V. This gap was possible to detect given the massive amount of red dwarfs detected by the satellite (more than 250.000 sources). From the theoretical perspective, Baraffe & Chabrier (2018) and MacDonald & Gizis (2018) relate the gap to a complex interplay between the production of ^{3}He and its transport by convection. With a vast amount of high-quality data, the Hertzsprung-Russell diagram could thus provide a deep insight into the interior structure of low mass stars.

4. Substellar formation scenarios and observational constrains

Currently the substellar formation mechanisms scenario counts with five main theoretical proposals: hierarchical fragmentation (Bonnell et al., 2008), gravoturbulent fragmentation (Padoan & Nordlund, 2004), disc fragmentation (Bate et al., 2002, 2003; Goodwin et al., 2004), ejection of protostellar embryos (Reipurth & Clarke, 2001) and photo erosion (Hester et al., 1996; Whitworth & Zinnecker, 2004). There are different observational constraints to the theoretical models: the shape of the low-mass initial mass function and its minimum mass, (sub)stellar multiplicity, spatial and kinematic distributions at birth, prevalence and sizes of circum(sub)stellar disks and envelopes and, the dependence of these properties on the star-forming environment.

Changes in the shape of the initial mass function, independently of its functional form, are related with different dominant formation processes in a given mass regime. For substellar sources, there has been a steady effort in nearby young star-forming regions trying to asses its impact in the mass function (system initial mass function). There is a consensus of a universal initial mass function down to the $\sim$0.03 $\mathrm{M_\odot}$, described as a lognormal distribution it would have a characteristic mass around the 0.25 $\mathrm{M_\odot}$ and σ $\sim$0.5. Under the mentioned conditions the initial mass function in different young star-forming regions is consistent among each other within the quoted uncertainties. Various initiatives have tried to preserve uniformity of analysis in terms of instrumentations, study, applied corrections (e.g., mass segregation) and used models for the mass-luminosity relationship (de Wit et al., 2006; Moraux et al., 2003,

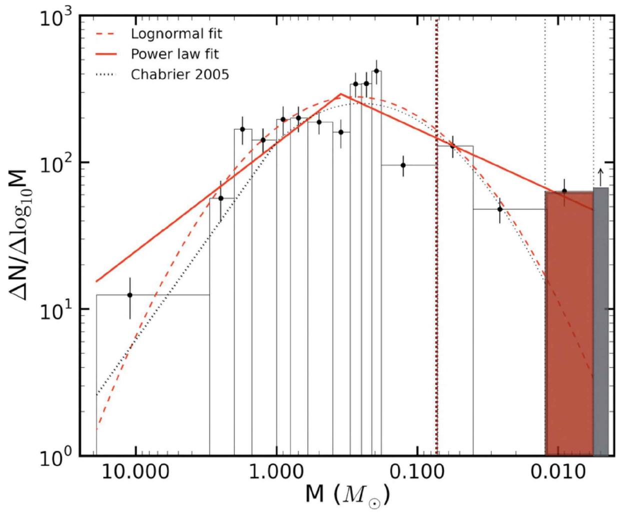

Figura 3: The σ Orionis mass function. The best lognormal fit to our data is depicted with a dashed line, the double power-law fit from our mass spectrum is illustrated with a continuous line, and the Chabrier (2005) mass function normalized to the total number of sources is plotted as a dotted line. Vertical error bars stand for the Poisson uncertainties. The highlighted mass bins account for the new substellar candidate members. Vertical dashed lines represent the classical stellar/substellar regime, the planetary mass regime and, our completeness level. Figure from Peña Ramírez et al. (2012).

2007; Scholz et al., 2009, 2012, 2013; Mužić et al., 2011, 2012, 2014, 2015). At lower masses, below the $0.03\,\mathrm{M}_\odot$ there is uncertainty in the initial mass function variations and its low-mass cut-off. Residual contamination, incompleteness, mass segregation and substantial uncertainties in the mass-luminosity relationship account among the factors that affect any assessment about the mass function shape at such low masses.

The case of the σ Orionis cluster ($\sim$3 Myr, $\sim$400 pc) is representative. The most recent study of its mass function (Peña Ramírez et al., 2012) used about 400 sources to cover the cluster mass range 19-0.004 $\mathrm{M}_\odot$ in an area of about 2800 arcmin^2, see Fig. 3. The discovery of 23 new sources as substellar members that gave hints of variations in the mass function below the $0.03\,\mathrm{M}_\odot$ led to an observational effort concluded in Zapatero Osorio et al. (2017), where about the half of those new candidates were confirmed as young clusters members given its optical and near-infrared spectra as seen in Fig. 4. For the faintest cluster candidate members, the T-type sources identified in the cluster line of sight, the studies of Peña Ramírez et al. (2011, 2015) shows that none of the T-dwarfs is a possible σ Orionis member. Either planetary-mass objects with masses below $\sim 4\,\mathrm{M}_\mathrm{Jup}$ may not exist free-floating in the cluster, or they may lie at fainter near-infrared magnitudes than those of the targets (i.e., $H > 20.6$ mag), thus remaining unidentified to date.

Another observational constraint to the substellar formation scenarios looks for its dependence on star-forming environments. In that sense the work of Mužić et al. (2017) focusses on RCW38 ($\sim$1 Myr, $\sim$1.7 kpc, $\sim$300 sources), a dense environment

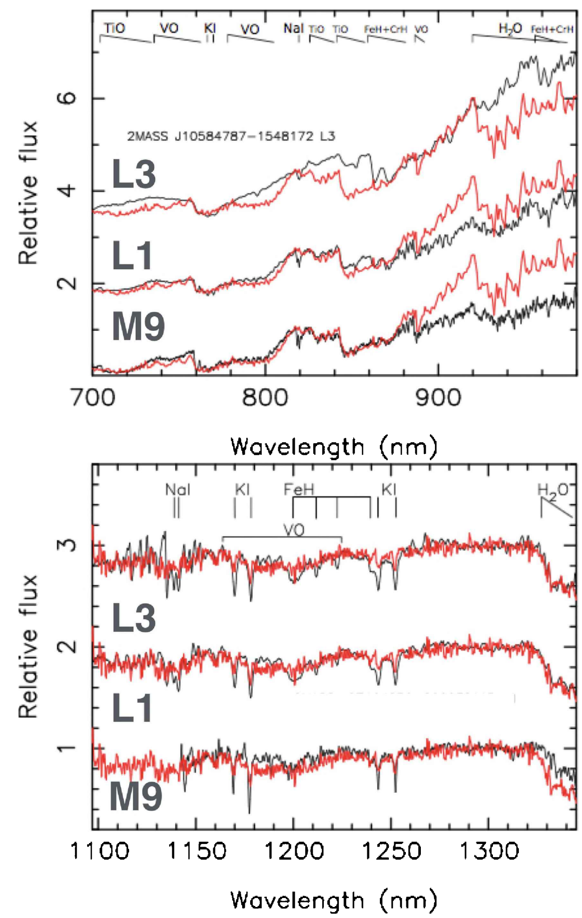

Figura 4: Combination of all spectroscopic data in optical and near-infrared of the faintest σ Orionis members, shown in red. The field high-gravity spectral standards are plotted as black lines. All spectra have the same wavelength resolution for a proper comparison. The most prominent features are labeled. Optical and near-infrared spectra are normalized to unity at 814-817.5 nm and 1.28-1.32 μm. The data are vertically shifted by a constant. Figure from Zapatero Osorio et al. (2017).

(2500 pc^{-2}), twice denser than the Orion Nebular Cluster or 10 times denser than NGC1333. Their results are in agreement with the values found in other young star-forming regions, revealing no evidence that a combination of high stellar densities and the presence of numerous massive stars affect the formation efficiency of brown dwarfs and very-low-mass stars. An ongoing effort, under the same premise, is focussed in the young massive cluster NGC2244 ($\sim$2 Myr, $\sim$1.6 kpc), located in the Rosette nebula (Mužić et al., 2019).

Broadly speaking, to obtain an initial mass function a luminosity function must be derived, using a mass-luminosity relation and applying the relevant corrections due to the dynamical evolution and multiplicity of the members. There are a series of caveats that arise in the process. In terms of the mass-luminosity relation, there is a direct dependence on the theoretical uncertainties and models are tied to a specific age, distance, and metallicity. The theoretical treatment of the low mass is homogeneous, therefore claims about the accretion history affecting the early stellar evolution for ages less than 10 Myr is usually not taken into account (Baraffe et al., 2017). Effects such as rotation will inflate the radius determination and therefore modify the inferred luminosity value. Also at including magnetic activity, it can be produced cool spots reducing the T_{eff} and consequently the mass estimation.

Regarding corrections of dynamical evolution, effects such as mass segregation and loss of low-mass members can impact the mass function derivation, although usually it is not considered when dealing with very young environments. Deriving the luminosity function requires a large sample of clean members, deal with contaminants, completeness, and extinction plus it needs to understand the processes of conglomerate assembly, equilibration, and dissolution. Additionally, the source movements in the youngest environments should reflect the dominant conglomerate formation process. At this stage, it therefore critical to fully account the entire population of interest.

5. A wider view

Just until recently ultra-cool dwarf studies in substellar/stellar conglomerates (e.g., young star-forming regions, associations, young moving groups) have been mapped under the limitation of relatively small field coverage. Telescopes such as VISTA at Paranal, Chile have been able to map uniformly in the near-infrared vast regions of different star forming regions and open clusters with surveys such as Vista Variables de la Vía Láctea (eXtended) (Minniti et al., 2010) VVV(X) or the VISTA Star Formation Atlas (VISIONS) which is focused in the ultra-cool dwarf population of various star-forming complexes. When completed, VISIONS will be the most sensitive and complete near-infrared survey of local star formation and will feed the next generation of telescopes with new targets for star and planet formation studies. Alternative approaches such as the Dynamical Analysis of Nearby ClustErs (DANCE, Bouy et al., 2013) aimed at deriving a comprehensive and homogeneous census of the stellar and substellar content of a number of nearby (<1 kpc) young (<500 Myr) associations re-reducing in an uniform manner data from different facilities to increase spatial coverage offers combined multi-epoch deep wide field images.

In the last year, with the advent of Gaia DR2 data, the concept of a wider view mapping substellar/stellar conglomerates achieved a new level. For example in the Vela OB2 region ($\sim$10 Myr, $\sim$336 pc), the first surveys with contoured X-ray data gave a selection of pre-main sequence stars with lithium detections (Pozzo et al., 2000). Studies in a larger area like the ones presented by Jeffries et al. (2014) and Sacco et al. (2015) shows evidence of a bimodal radial velocity distribution, product of a mixed population with a nearby structure. Last year only, using Gaia DR2 data, Franciosini et al. (2018) confirmed two populations separated $\sim$38 pc from each other along our line of sight. Beccari et al. (2018), in a 10 $\times$ 5 deg^2 field conclude that there are stars of the age of Vela OB2 plus four different subgroups. Cantat-Gaudin et al. (2018), have confirmed the subclustering, updated the mass budget of the conglomerate from $\sim$1000 $M_\odot$ to $\sim$2330 $M_\odot$, connect the complex with the IRAS Vela Shell as well as conclude that there is no presence of mass segregation effects. Even at lower masses ($\sim$0.16 $M_\odot$) the work of Armstrong et al. (2018) using previously known low mass members in a small region of Vela OB2, designed a selection criteria that combine Gaia and 2MASS photometry, independently of any astrometric information, to identify low-mass stars detecting a widespread population across the whole area of the association. The authors claim that there are apparent differences in the spatial distributions of the low-mass and the high-mass OB populations, suggesting either that the structure and dynamics of these populations have evolved separately or that the initial mass function can vary considerably on small scales within a single association.

The Scorpius-Centaurus OB2 region ($\sim$5-11 Myr, $\sim$120-160 pc) is another conglomerate where a wider view has given us exciting results. Given its large extension ($\sim$2000 deg^2), this complex of B-type stars is usually referred to as an association. To derive a complete mass function in such a vast region is a challenge. It is separated in the Upper Scorpius, Upper Centaurus Lupus and Lower Centaurus Crux regions. Nevertheless, the work of Damiani (2018), presents a spatial density map indicating the boundaries of the traditional conglomerates known in Scorpius-Centaurus OB2 plus enhanced low-density areas. This gives a new picture of the region with a series of new clusters identified within the main conglomerate(s). Authors conclude that kinematically diffuse groups are older whereas compact groups are younger with a significant age spread among the groups. At lower masses ($\sim$0.02 $M_\odot$) in Lower Centaurus Crux, the study of Goldman et al. (2018) add about 1800 new intermediate- and low-mass young stellar objects and brown dwarfs, that escaped identification until Gaia DR2. The discoveries will add up to a total mass of about 700 $M_\odot$ in the complex, grouped the new members in four denser subgroups, which have an increasing age from 7 to 10 Myr, surrounded by "free-floating" young stars with mixed ages. In the case of the Upper Scorpius region, the survey of Luhman (2018) adds more than a thousand of additional low mass candidate members to the region. The census now encompasses a large portion of early L dwarfs, excluding the ρ Ophiuchus star-forming region.

Finally, one of the most studied star-forming regions, the Orion complex, has also been recently revisited with a wider perspective. The study of Großschedl et al. (2018) uses the Gaia DR2 distances of about 700 mid-infrared selected young stellar objects in the benchmark giant molecular cloud Orion A to infer its 3D shape and orientation. These authors find a denser and enhanced star-forming (bent) *head*, and a lower density and star-formation quieter $\sim$75 pc long *tail* across the area studied. With this results, Großschedl et al. (2018) find that the current cloud and young stellar object masses toward the *tail* can be underestimated by about 30 % to 40 % under the common assumption of a single constant distance to Orion A. Also very recently, Briceno et al.

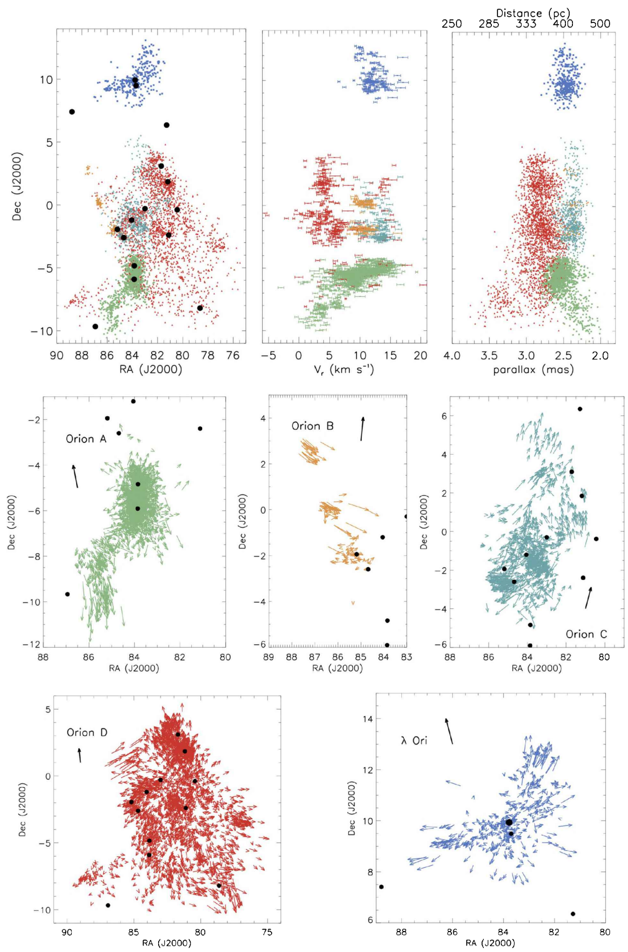

Figura 5: Distribution of stars identified as members Orion A (green), Orion B (orange), Orion C (cyan), Orion D (red), and λ Ori (blue). Proper motions of the stars identified as members of the complex, relative to the average proper motion in each structure are also shown. The length of the vectors correspond to the motion of over 1.2 Myr. Figure from Kounkel et al. (2018).

(2018) pursued a vast photometric study ($\sim$180 deg^2) across the Orion OB1 association, complemented with extensive follow up spectroscopy. They mapped and characterized the off-cloud, low-mass, pre-main sequence populations uniformly. Their main conclusion is that the spatial distribution of the young stars across Orion OB1 is far from uniform, but rather has a significant degree of substructure. This feature has also been acknowledged in the work of Kounkel et al. (2018). Using together physical information from Gaia DR2 and the Apache Point Observatory Galactic Evolution Experiment (APOGEE Gunn et al., 2006; Blanton et al., 2017) spectrograph, the authors gave an unprecedented 6-dimensional view of the entire Orion complex as can be seen in Fig.5. It was possible the identification of spatially and kinematically distinct groups of young stellar objects with ages ranging from 1 to 12 Myr. Among other results, two separate populations towards OriOB1 (d, RV) were identified: Orion C (3 formation epochs, 2-10 Myr, σ Orionis associated) and Orion D. Both spans the full extent of the OB1ab region. There were also found several peculiar substructures, the radial expansion of λ Orionis was confirmed as well as the movement of various groups in Orion B towards NGC 2024.

Agradecimientos: I gratefully acknowledge the local organizers and staff members of the Second Binational Meeting AAA-SOCHIAS meeting for all the work done. I also acknowledge CONICYT PAI Concurso Nacional de Inserción en la Academia, Convocatoria 2016 Folio PAI79160052.

Referencias

Allard F., 2014, M. Booth, B.C. Matthews, J.R. Graham (Eds.), *Exploring the Formation and Evolution of Planetary Systems, IAU Symposium*, vol. 299, 271–272
Allard F., Homeier D., Freytag B., 2012, Philosophical Transactions of the Royal Society of London Series A, 370, 2765
Alves J., Bouy H., 2012, A&A, 547, A97
Alves de Oliveira C., et al., 2013, A&A, 549, A123
Apai D., et al., 2017, Science, 357, 683
Ardila D., Martín E., Basri G., 2000, AJ, 120, 479
Armstrong J.J., Wright N.J., Jeffries R.D., 2018, MNRAS, 480, L121
Baraffe I., Chabrier G., 2018, A&A, 619, A177
Baraffe I., et al., 1998, A&A, 337, 403
Baraffe I., et al., 2015, A&A, 577, A42
Baraffe I., et al., 2017, A&A, 597, A19
Barrado y Navascués D., et al., 2007, ApJ, 664, 481
Bate M.R., Bonnell I.A., Bromm V., 2002, MNRAS, 332, L65
Bate M.R., Bonnell I.A., Bromm V., 2003, MNRAS, 339, 577
Bayo A., et al., 2011, A&A, 536, A63
Beccari G., et al., 2018, MNRAS, 481, L11
Best W.M.J., et al., 2017, ApJ, 837, 95
Best W.M.J., et al., 2018, ApJS, 234, 1
Bihain G., et al., 2009, A&A, 506, 1169
Blanton M.R., et al., 2017, AJ, 154, 28
Bonnell I.A., Clark P., Bate M.R., 2008, MNRAS, 389, 1556
Bouy H., et al., 2013, A&A, 554, A101
Briceno C., et al., 2018, arXiv e-prints
Burgess A.S.M., et al., 2009, A&A, 508, 823
Caballero J.A., et al., 2007, A&A, 470, 903
Cantat-Gaudin T., et al., 2018, arXiv e-prints
Chabrier G., 2005, E. Corbelli, F. Palla, & H. Zinnecker (Ed.), *The Initial Mass Function 50 Years Later, Astrophysics and Space Science Library*, vol. 327, 41
Chambers K.C., et al., 2016, arXiv e-prints
Chiang P., Chen W.P., 2015, ApJL, 811, L16
Crossfield I.J.M., et al., 2014, Nature, 505, 654
Damiani F., 2018, A&A, 615, A148
de Wit W.J., et al., 2006, A&A, 448, 189
Dieterich S.B., et al., 2018, ApJ, 865, 28
Esplin T.L., et al., 2017, AJ, 154, 46
Franciosini E., et al., 2018, A&A, 616, L12
Gagné J., Faherty J.K., 2018, ApJ, 862, 138
Gaia Collaboration, et al., 2018, A&A, 616, A1
Geers V., et al., 2011, ApJ, 726, 23
Goldman B., et al., 2018, ApJ, 868, 32
Goodwin S.P., Whitworth A.P., Ward-Thompson D., 2004, A&A, 414, 633
Großschedl J.E., et al., 2018, A&A, 619, A106
Gunn J.E., et al., 2006, AJ, 131, 2332
Hester J.J., et al., 1996, AJ, 111, 2349

Hillenbrand L.A., Hoffer A.S., Herczeg G.J., 2013, AJ, 146, 85
Ingraham P., et al., 2014, ApJ, 782, 8
Jao W.C., et al., 2018, ApJL, 861, L11
Jeffries R.D., et al., 2014, A&A, 563, A94
Kounkel M., et al., 2018, AJ, 156, 84
Lodieu N., et al., 2018, MNRAS, 473, 2020
Lucas P.W., et al., 2001, MNRAS, 326, 695
Luhman K.L., 2013, ApJL, 767, L1
Luhman K.L., 2018, AJ, 156, 271
Luhman K.L., Esplin T.L., Loutrel N.P., 2016, ApJ, 827, 52
Luhman K.L., et al., 2006, ApJ, 647, 1180
MacDonald J., Gizis J., 2018, MNRAS, 480, 1711
Minniti D., et al., 2010, NewA, 15, 433
Moraux E., et al., 2003, A&A, 400, 891
Moraux E., et al., 2007, A&A, 471, 499
Mužić K., et al., 2011, ApJ, 732, 86
Mužić K., et al., 2012, ApJ, 744, 134
Mužić K., et al., 2014, ApJ, 785, 159
Mužić K., et al., 2015, ApJ, 810, 159
Mužić K., et al., 2017, MNRAS, 471, 3699
Mužić K., et al., 2019, Apj. Submitted
Padoan P., Nordlund Å., 2004, ApJ, 617, 559
Peña Ramírez K., Béjar V.J.S., Zapatero Osorio M.R., 2016, A&A, 586, A157
Peña Ramírez K., Zapatero Osorio M.R., Béjar V.J.S., 2015, A&A, 574, A118
Peña Ramírez K., et al., 2011, A&A, 532, A42
Peña Ramírez K., et al., 2012, ApJ, 754, 30
Pozzo M., et al., 2000, MNRAS, 313, L23
Reipurth B., Clarke C., 2001, AJ, 122, 432
Reylé C., 2018, A&A, 619, L8
Sacco G.G., et al., 2015, A&A, 574, L7
Scholz A., et al., 2009, ApJ, 702, 805
Scholz A., et al., 2012, ApJ, 744, 6
Scholz A., et al., 2013, ApJ, 775, 138
Scholz R.D., Bell C.P.M., 2018, Research Notes of the American Astronomical Society, 2, 33
Slesnick C.L., Carpenter J.M., Hillenbrand L.A., 2006, AJ, 131, 3016
Suárez G., et al., 2017, AJ, 154, 14
Suenaga T., et al., 2014, PASJ, 66, 33
Weights D.J., et al., 2009, MNRAS, 392, 817
Whitworth A.P., Zinnecker H., 2004, A&A, 427, 299
Zapatero Osorio M.R., Béjar V.J.S., Peña Ramírez K., 2017, ApJ, 842, 65
Zapatero Osorio M.R., et al., 2000, Science, 290, 103